The 7th World Congress on Particle Technology (WCPT7)

Influence of granule porosity during fluidized bed spray granulation

Torsten Hoffmann[a*], Christian Rieck[a], Andreas Bück[a], Mirko Peglow[b],

Evangelos Tsotsas[a]

[a]*NaWiTec, Thermal Process Engineering, Otto-von-Guericke University, Universitätsplatz 2, Magdeburg, 39106, Germany*
[b]*Pergande GmbH, Wilfried Pergande Platz 1, Weißandt-Gölzau, 06369, Germany*

Abstract

Fluidized bed spray granulation is an important process for the transformation of liquids into solid materials. Especially product properties like final particle size and structure of the granules are important. These properties are closely related to the selected process parameters such as temperature and spraying rate. By knowing the relationship between the thermal process conditions and resulting particle structure, the final product can be designed according to the wishes of the consumers. In the presented work, a correlation between the thermal process conditions and the achieved shell porosity, which is relevant for the particle structure, is revealed. Therefore two experimental series with different materials (non-porous glass particles and porous alumina) were performed in a lab-scale fluidized bed spray granulator. The lab-plant allows the precise measurement of the inlet and outlet temperatures and moisture contents of the gas. All process parameters were kept constant except the inlet gas temperature and the spraying rate. Although the amount of initial material as well as the amount of injected solution was the same for all experiments, the final particle size distribution and the structure of the formed shell were clearly different. The obtained experimental results were compared with a process model including a new expression for the growth kinetics, which takes into account an acceleration of the growth velocity due to the formation of a porous structure. The used model also considers the separation of the fluidized bed into two different zones, namely the spraying zone and the drying zone. With the given initial process conditions, the model calculates the time evolution of the particle size distribution, the theoretical outlet temperature and the moisture content of the gas. The introduction of the shell porosity into the growth kinetics reduces the underestimation of the particle size in the model, which occurs if the formed layer on the particle surface is assumed to be compact.

* Corresponding author. Tel.:+86-13808694306; fax: +64 6 3505241.
  E-mail address: Torsten.Hoffmann@ovgu.de

1. Introduction

Approximately 60% of all industrially goods are particulate solids [1] because the handling, storing and further processing is often easier than for liquid substances. One fundamental process for the fabrication of granular products is fluidized bed spray layering granulation (FBSG), especially in food and pharmaceutical industries. Depending on the large variety of application very different particles are needed. The process of FBSG offers the advantage of a selective control of product properties such as particle size, moisture content, solubility or composition by forming it out of, e.g., suspensions, solutions, emulsions or melts. Furthermore the porosity or rather the structure of the granules can be influenced by the chosen process conditions.
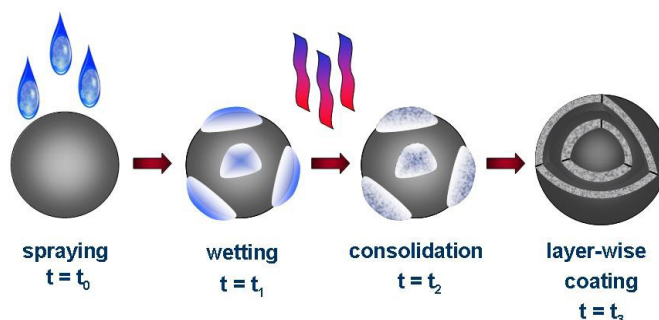

Fig. 1.Granulation scheme.

The following cases should provide a short overview. If an active substance should have a fast release then a porous surface is preferred. But also the opposite case of a compact and smooth surface is possible. These coated particles were used e. g. to protect the core from outer influences for a certain time. Often very narrow particle size distributions are preferred by the costumer but in some cases wide distributions offer more benefits. To that reason the FBSG-user has to know which process parameter to choose to handle the process in the right way and to push the product quality in the favored direction. For a better understanding, a closer look on the micro-phenomena is necessary. The primary particles which are used as seeds during the granulation can consist out of filling material or even the active component itself from an industrial point of view. These seeds are streamed by hot gas to fluidize them. Out of a nozzle, which can be positioned on the bottom, side or top of the process chamber, droplets are sprayed on the particles. The differences in deposition, spreading, penetration and drying of the droplets will affect the process development and yield to different particle properties. The challenge is to predict all these phenomena (Fig. 1) in detail. So a fundamental understanding, of how it is possible to produce such different product properties with the same material and the same apparatus, is needed. The investigation of how the process conditions influence the particle porosity is done experimental. Macroscopic population balance equations (PBE) are enhanced and tested with the derived influences from the experimental investigations. The modeling of such a complex granulation process is split in two main parts. The first one is the description of the temporal evolution of the particle size distribution. For the case of describing only one characteristic parameter, namely the particle size x, the layering process can be described by a one-dimensional PBE. The second part is the description of the drying conditions. The dependency of the achieved granule porosity on the thermal process conditions is expressed by an empirical correlation which is established from experiments. Results for both are presented and discussed in section 4.

2. Modeling

2.1. Population balance mode (PBE)l

Beside the assumption of describing only the evolution of the particle size distribution no particle breakage, no agglomeration and no overspray shall appear. This means that all solution with is sprayed in the process will remain on the particles in the fluidized bed. With the taken assumptions, the ordinary PBE for a batch process results in

$$\frac{\partial n}{\partial t} = -\frac{\partial \overline{G} n}{\partial x}.$$ (1)

Because of fluid dynamic measurements in a 2D fluidized bed [2], which show a separation of the fluidized bed in different zones, the growth model approach by Heinrich et al. [3] was more generalized. The apparatus was split in two different zones (see Fig.2), namely into an active spraying zone and a passive drying zone.
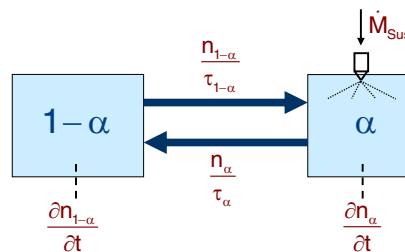

Fig. 2. Scheme of the two-zone model with drying zone (left) and spray zone (right).

Thus the PBE for the spraying zone, where particle growth beside drying occurs, is

$$\frac{\partial n_\alpha}{\partial t} = -\frac{\partial \overline{G} \cdot n_\alpha}{\partial x} - \frac{n_\alpha}{\tau_\alpha} + \frac{n_{1-\alpha}}{\tau_{1-\alpha}},$$ (2)

and the PBE for the drying zone, where only particle drying occurs is

$$\frac{\partial n_{1-\alpha}}{\partial t} = \frac{n_\alpha}{\tau_\alpha} - \frac{n_{1-\alpha}}{\tau_{1-\alpha}},$$ (3)

where τ_α, $\tau_{1-\alpha}$ are the mean residence times of the particles in the zones. In fact, the possible formation of different particle porosities is not explicit in this model approach. The consideration of the formation of different particle porosity is integrated in a novel approach for the growth kinetics.

2.2. Kinetic of the population balance

The growth kinetic for the FBSG process is strongly related to the way of droplet deposition on the single particles. Uhlemann et al. [4] assumed that the droplets which were injected by the nozzle are deposited on the particles according to the surface area of each particle. The assumption implies that the liquid film on the particle surface, which is formed out of the droplets, has the same thickness for each granule. This leads to

$$\overline{G} = \frac{2 \cdot \dot{M}_{sus,s}}{\rho_s \cdot A_{bed}},$$ (4)

which is independent of the particle size. It only depends on the spraying rate $\dot{M}_{sus}$, the density of the solid ρ_s and on the total particle surface A_{bed}. For cases when the liquid film on smaller particles is thicker than on larger ones or for the opposite case, the growth rates depend on the particle size. To consider these effects the prior approach was modified by the assumption that the deposition of droplets on the granules can be proportional to an arbitrary moment or any linear combination of different growth kinetics,

$$\overline{G} = \sum_{i=0}^{l} \lambda_i \cdot G_{\varepsilon,i}, \tag{5}$$

whereby the summation of the coefficients λ_i has to yield unity. The formation of different shell porosities ρ_{sh} for the growth kinetic is included in

$$G_{\varepsilon,i} = \frac{2 \cdot \dot{M}_{sus,s} \cdot x^{i-2}}{\rho_{sh} \cdot \mu_i} \qquad (6), \text{ with } \mu_i = \int_0^\infty x^i \cdot n \; dx. \tag{7}$$

The novel approach considers the flexible droplet deposition and the existence of diverse shell porosities. Higher shell porosity will lead to higher growth rates. The prior assumptions were also considered as limiting cases. For the case that the index i=2 and the shell porosity ρ_{sh} is zero the growth rate can be converted into the previous approach:

$$G_{\varepsilon,i} = \frac{2 \cdot \dot{M}_{sus,s} \cdot x^{i-2}}{\rho_s \cdot (1 - \varepsilon_{sh}) \cdot \mu_i} = \frac{2 \cdot \dot{M}_{sus,s}}{\rho_s \cdot A_{bed}} \tag{8}$$

2.3. Drying conditions

The modeling of the drying conditions is, beside the description of droplet deposition on the particle surface the second important part to predict the particle growth during the FBSG process. The process conditions influence the way of the droplet drying and therefore the formation of different granule porosity. Process parameters like inlet temperature, process gas mass flow and spraying rate have a great impact to the drying velocity of the liquid droplets. This drying speed influences if either porous or nonporous granules arises. All these parameter that manipulate the drying speed can be considered in one factor, namely the dimensionless drying potential

$$\eta = \frac{\left(Y_{sat} - Y_{out}\right)}{\left(Y_{sat} - Y_{in}\right)}. \tag{9}$$

The dimensionless drying potential is the division of the still evaporable amount of water through the maximal evaporable amount of water. For the case that the outlet moisture content is dry, the drying potential will tend towards unity. Consequently the drying potential will be zero if the gas is saturated. Furthermore, $1-\eta$ can be interpreted as gas-side drying efficiency.

3. Experimental setup

Experiments were conducted to investigate the process parameter influences of temperature and spraying rate on granule porosity. For that reason, a well-define coating process was realized in a small lab-scale coating granulator (GLATT GmbH type GCPG-1.1). A small scheme and a photo are shown in Fig. 3. The granulation experiments have been carried out batch-wise while only one parameter is varied between the different trials. The GCPG equipment was modified corresponding to the experimental needs. The cylindrical process chamber has a diameter of 150 mm and a two-component nozzle of Schlick GmbH installed in top-spray configuration. The tip of the nozzle has an opening diameter of 0.8 mm and position number two was taken for the air distributor cap, to get a homogeneous, finely-dispersed spray. Compressed air is used for nozzle air supply and also for the fluidization gas

itself. So conditions of the inlet air are very stable, especially dew point temperature and the mass flow rates. The mass flow rates were recorded by mass flow meters of Bronkhorst-Mättig Company, type F-106BI and F-112AC. Inlet, bed and outlet temperatures were measured as well as inlet and outlet moisture content. The moisture content of the air was measured by two Infrared spectrometers of Fisher-Rosemount Company, type NGA 2000 MLT3. All analog signals were converted in digital ones by a data logger and visualized and recorded every two seconds by the software DasyLab. All dust from the exhaust air is cleaned by an internal filter at the top of process chamber. With the outlet gas flap it is possible to change the pressure in the fluidized bed chamber. This is necessary to secure constant conditions for the measurement of inlet and outlet moisture
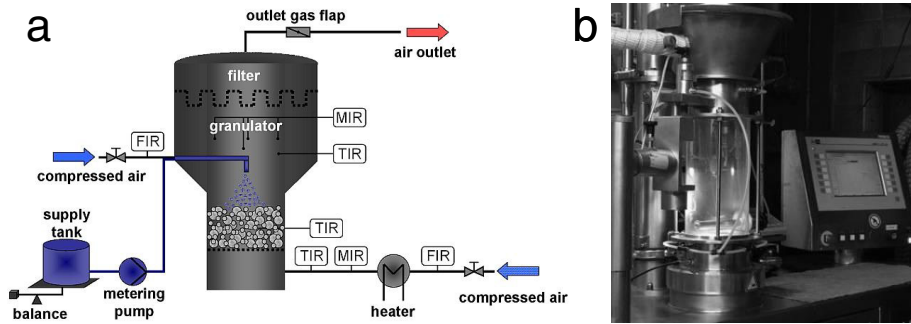

Fig. 3. (a) scheme and; (b) photo of experimental plant.

For the granulation experiments the material should have a high sphericity. So glass zirconia beads and γ-alumina beads were used as seeds (Tab. 1). The glass beads Type GZ (0.5 - 0.8mm) supplied by Sigmund Lindner GmbH are non-porous and non-hygroscopic. The γ-alumina beads supplied by Sasol Company are porous and hygroscopic, so that two completely different materials were tested.

Table 1. Material properties of γ-Alumina and glass beads.

Material parameters	γ-Alumina	glass beads
sauter mean diameter [mm]	0.62	0.49
sphericity [-]	0.97	0.94
particle density [kg/m³]	1280	2400

As coating material sodium benzoate was used. Because of the very good solubility in water, high solid concentrations are possible (30 wt%). Furthermore, it is also easier to clean the equipment using pure water only. Sodium benzoate is a white crystalline salt, known as E211, which is mostly used in industries as a conservation material. As said before only inlet temperature and spraying rate are varied. Moreover the fluidization flow rate had to be change from 75 kg/h for the γ-alumina beads up to 120 kg/h for the glass beads and the hold up from 0.5 kg to 1 kg, because of the higher particle density. But all other process parameters like total amount of sprayed solution (1 kg), nozzle air mass flow (1.68 kg/h) were kept always the same (see all process parameters in Table 2).

The structure of the product particles and the porosity of the shell were analyzed by using using a micro x-ray computed tomography device (μ-CT) of Procon X-Ray Company. It allows the analysis of geometric structures in three dimensions, so detection of inner pores and voids is possible. The maximal resolution is about 0.6 μm and the evaluation of the recorded volume images was performed by MAVI software of the Fraunhofer Institute for Technical and Industrial Mathematics Kaiserslautern. The measurement of the shell porosity was possible because density difference between core and shell yields to differing grey values and with the help of MAVI software the shell was separated from the core (see Fig. 4). Finally the porosity of the shell is calculated by the usage of different graphical filters and mathematical operations [5].

Table 2. measured and calculated process parameters.

| No.	Material	$T_{g,in}$ [°C]	$T_{g,out}$ [°C]	$Y_{g,in}$ [g/kg]	$Y_{g,out}$ [g/kg]	$Y_{g,sat}$ [g/kg]	M_{gas} [kg/h]	M_{sus} [g/h]	η [-]	ε_{sh} [-]
1	glass	50	40.8	1	3.5	12.7	120	500	0.79	0.497
2	glass	50	34.1	1	6.1	12.7	120	952	0.56	0.638
3	glass	95	80.8	1	3.6	24.6	120	517	0.89	0.463
4	glass	95	70.1	1	7.6	24.4	120	1310	0.72	0.504
5	γ-Al$_2$O$_3$	50	37.0	1	5.6	13.1	75	505	0.62	0.612
6	γ-Al$_2$O$_3$	50	25.2	1	10.9	13.5	75	1128	0.21	0.684
7	γ-Al$_2$O$_3$	95	80.0	1	5.3	25.7	75	507	0.83	0.527
8	γ-Al$_2$O$_3$	95	65.4	1	10.6	25.4	75	1084	0.61	0.646
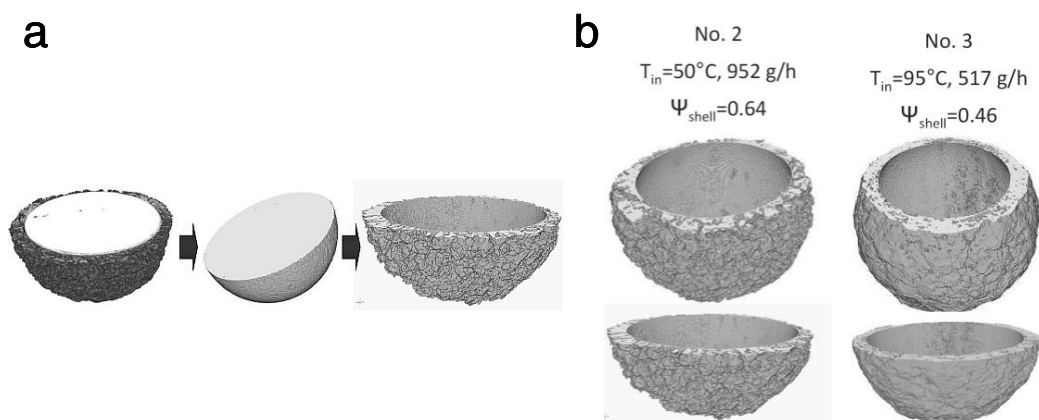
Fig. 4. (a) Step wise separation of the granule; (b) Micro-CT measurement for different shell porosities.

The temporal evolution of the particle size distribution was determined using a particle size analyzer (Camsizer) of Retsch Company. Therefore at the beginning and at the end of each experiment samples were taken and analyzed off-line [6].

4. Results and discussion

The comparison in Fig. 5 between the Micro-CT measurements for the shell porosities and the corresponding drying conditions, in the form of the dimensionless drying potential, show a clear and almost linear trend. The larger the dimensionless drying potential, the lower is the shell porosity of the final particles. Furthermore an explicit difference between both materials is obvious. The linear trend for γ-alumina does not have such a large slope than the glass material. The reason for that could be due in the different porosities and hygroscopicity of the primary materials. This could lead to different infiltration rates for the droplets. For both materials an empirical correlation were established by a linear fit of the measured shell porosities and the calculated dimensionless drying potentials. For the γ-alumina beads the extracted correlation is

$$\varepsilon_{sh} = f(\eta) = -0.23\eta + 0.75. \tag{10}$$

and for the glass beads

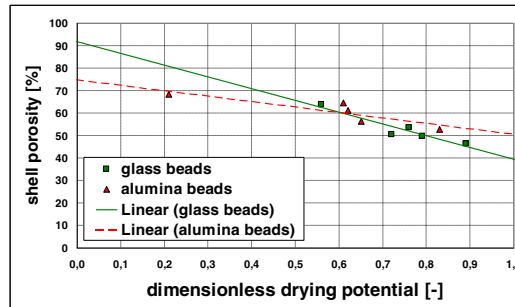$$\varepsilon_{sh} = f(\eta) = -0.53\eta + 0.92. \tag{11}$$

Fig. 5. Relationship between granule porosity and drying conditions

To understand the phenomena how different drying conditions lead to changes in the shell porosity a discussion of the process of changing from a liquid droplet to solid is necessary. Sodium benzoate which was used for the coating is a salt, so it is more or less a crystallization process when the droplet turns from liquid to solid. The crystallization process consists of two main steps: The nucleation step and the crystal growth step. Both steps are counter-acting and depend on the salt concentration in the solution. First of all, the concentration has to reach saturation, before crystallization takes place. Below this critical value, all crystals will dissolve again. After reaching the critical concentration, suddenly nucleation takes place. To receive a stable crystallization, a certain seed size has to be reached. This seed size depends on the temperature. The higher the supersaturation, the higher is the amount of newly generated seeds. So for a high nucleation rate, high supersaturation is needed. For crystal growth, low values of oversaturation are needed. Transferring this to the droplet drying, the speed of drying becomes the main influence. If the droplet drying is quick the concentration in the droplet will increase fast and this lead to high oversaturation with the consequence of many small nucleation seeds. The generated crystals have no time to grow; it is more like a precipitation reaction. The small crystals will sediment on the particle surface and will form compact shell structures. If the droplet drying is slow, the increase of the concentration will take longer and the oversaturation is not so high. This will lead to a very good crystal growth and larger crystals will be generated. If these larger crystals sediment on the particle surface they will form rough and porous shell structures. So the velocity of droplet drying and the achieved crystallization is the reason for different granule porosities. Changing process parameters like spraying rate and temperature will directly change the velocity of droplet drying and by this the process of crystallization. In Fig. 6 six the two counter-acting steps in relationship to the dimensionless drying potential, which includes the main process parameters of droplet drying conditions, is shown by trend.
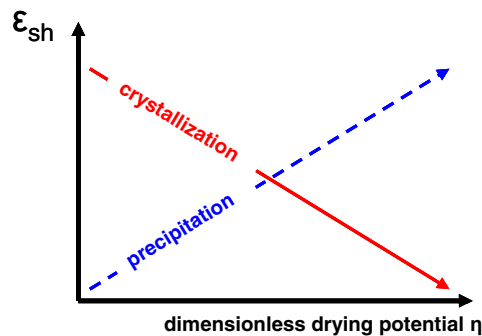
Fig. 6. Dependency of the counter-acting steps during crystallization form the dimensionless drying potential.

The novel process model approaches, which are introduced in section 2, were compared with the conducted experiments (see Fig. 7 and 8). In addition, the established empirical correlations (equation 10 and 11) were included. For solution of the one-dimensional PBE (2) and (3) they were transformed into a set of differential equations applying the flux limiter scheme of Koren [7] to prevent numerical diffusion effects. With the finite volume method [8] the differential equations were discretized. The resulting equations were implemented into the MATLAB programming environment. The chosen ode15s solver uses numerical differentiation formulas and is suitable for stiff problems [9].

The comparison in Fig. 7, between the simulated particle size distributions for the experiments with non-porous glass particles, shows a good agreement with the measured ones. The diagram on the left (a) shows the different particle growth that arises from the different drying conditions and thus different porosities. The diagram on the right shows despite various process parameters a similar particle growth, which is caused by the similar drying conditions and the similar porosities.
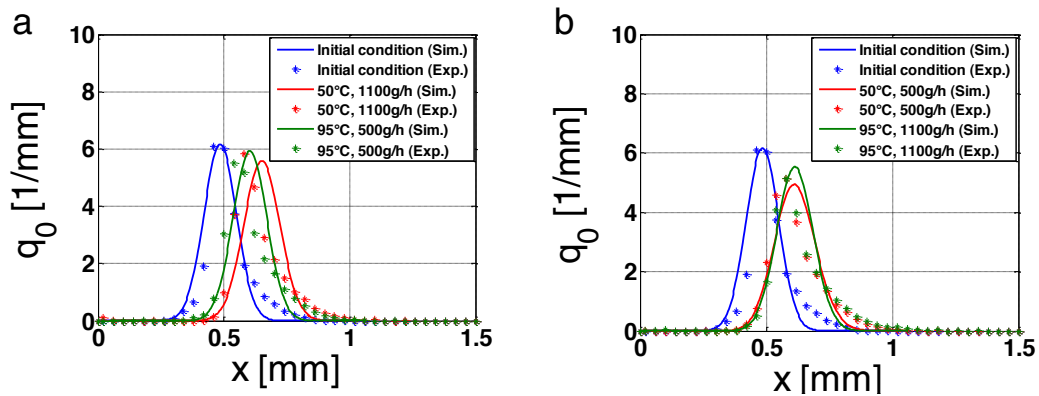

Fig. 7. Evolution of the particle size distribution with glass beads as seeds, (a) experiments with different and (b) with similar dimensionless drying potential

Fig. 8 shows the comparison between simulated and measured particle size distributions for the porous γ-alumina material. The presentation is the same as for the glass beads. On the left side, the experiments with different growth conditions and on the right side the experiments with similar growth conditions are compared. Although the particle size distribution have a very narrow standard deviation and the experimental peaks consist of only a few points it can be seen, that for this material the model fails to predict the final particle size distribution. In fact the particle growth is overpredicted in every simulation. Obviously the differing starting material properties like porosity and hygroscopicity of the initial particles have an influence on the particle growth. In the beginning of droplet deposition on the particles the hygroscopicity will lead to an imbibition of the sprayed liquid. This will result in a loss of sprayed material, which is placed into instead of on the particle. So the actual particle growth process will start with delay. The process model does not consider this effect and overestimation of shell porosity is easily possible.
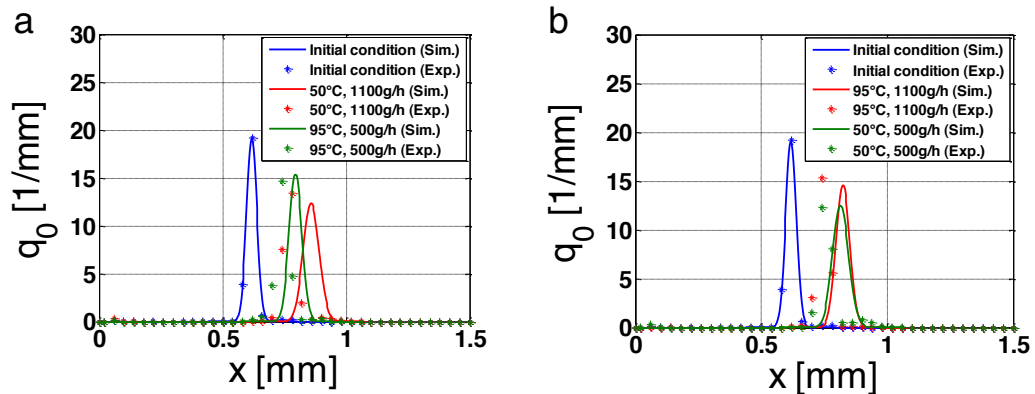
Fig. 8. Evolution of the particle size distribution with γ-alumina beads as seeds, (a) experiments with different and (b) with similar dimensionless drying potential

5. Summary and outlook

The experimental investigation of process parameters influencing the granule porosity showed that it is possible to generate with the same material different kinds of coating shells. A prior model approach was generalized to allow the possibility of this diversity. The influencing parameters were related to one factor, the dimensionless drying potential. This enables to evaluate which granule porosity will be generated when choosing a specific parameter configuration. The presented process model is able to predict the particle growth for non-porous materials. It was also explained what could be the reason for receiving different porosities by explaining the main effects in the crystallization process of the sprayed material. For porous particles the process model over predict the particle growth. One possible reason for this was given by the different porosities of the starting material but was not tested. The drying of single droplets on the two different starting materials might prove this approach.

Acknowledgements

Nomenclature	
A	particle surface
$\underline{G}$	particle growth rate
$\overline{G}$	linear combination growth rate
$\dot{M}$	spraying rate
n	particle number density
t	time
x	particle diameter
Y	moisture content of the fluidizing gas
α	volume fraction of the spray zone
ε	porosity
λ	linear coefficient
μ	moment of the number density distribution
η	dimensionless drying potential

ρ	density
τ	residence time

Indices

i	index i
in	inlet
gas	fluidization gas
out	outlet
s	solid
sat	saturation
sh	shell
sus	suspension
bed	fluidized bed

References

[1] D. Schulze, Pulver und Schüttgüter - Fließeigenschaften und Handhabung, Springer: Berlin Heidelberg New York, 2006.
[2] M. Börner, M. Peglow, M.S. van Buijtenen, N.G. Deen, E. Tsotas, J.A.M. Kuipers, Residence times in fluidized bed granulation, Abstracts & Proceedings WCPT6 (2010) ISBN: 978-3-00-030570-2.
[3] S. Heinrich, M. Peglow, M. Ihlow, M. Henneberg, L. Mörl, Analysis of the start-up process in continuous fluidized bed spray granulation by population balance modeling, Chemical Engineering Science 57 (2002), 4369-4390
[4] H. Uhlemann, Kontinuierliche Wirbelschicht-Sprühgranulation, Chemie Ingenieur Technik 62 (1990) 822–834.
[5] M. Dadkhah, M. Peglow, E. Tsotsas, Characterization of the internal morphology of agglomerates produced in a spray fluidized bed by X-ray tomography, Powder Technology Volume 228 (2012), 349-358.
[6] S. Heinrich, N. G. Deen, M. Peglow, M. Adams, J. Kuipers, E. Tsotsas, J. Seville, Measuring techniques for particle formulation processes. In Modern drying technology, Vol. 2: Experimental techniques, Wiley-VCH, Weinheim, 2009, 187–278.
[7] B. Koren, A robust upwind discretisation method for advection, diffusion and source terms, Numerical Methods for Advection-Diffusion Problems, Vieweg, Braunschweig, 2003.
[8] S. V. Patankar, Numerical heat transfer and fluid flow, Hemisphere Publishing Corporation, 1980.
[9] L. F. Shampine, M. W. Reichelt, The matlab ode suite, SIAM, Journal on Scientific Computing 18 (1997), 1–22.